Speed Control of 3-Phase Induction Motor in Presence of Sommerfeld Effect

A. Bisoi, R. Bhattacharyya and A.K. Samantaray

Abstract This paper considers the dynamics of an unbalanced rotor disk which is supported on a flexible foundation and is driven by a three-phase induction motor (IM). At resonance, the structural vibration amplitudes of the system are high and most of the motor power is spent to excite the structural mode of vibration. If the motor is improperly sized then it may not be possible for it to drive the rotor through this resonance. Even if the motor is sufficiently powerful, it first approaches the natural frequency and then suddenly jumps to a much higher value. This classic phenomenon is called the Sommerfeld effect. IM control laws often neglect this phenomenon. We develop a controller for such situation. The source-structure interaction involving the power transfer mechanism is modeled through bond graph and simulation results are presented.

Keywords Sommerfeld effect · Induction motor · Bond graph · V/f control

1 Introduction

During an experiment on an unbalanced motor placed on an elastic table, Arnold Sommerfeld came across a peculiar phenomenon. He found that near the structural resonance, there is considerable motor power consumption without much change in rotor speeds and at a critical power input, the motor speed jumps to a high value and keeps increasing with increase in voltage. This jump phenomenon was later named as Sommerfeld effect [1]. Sommerfeld effect at the stability threshold of a non-ideal system with DC motor was studied in [2, 3]. Bond graph technique [4] is very

A. Bisoi · R. Bhattacharyya (✉) · A.K. Samantaray (✉)
Indian Institute of Technology, Kharagpur, India
e-mail: rbmail@mech.iitkgp.ernet.in

A.K. Samantaray
e-mail: samantaray@mech.iitkgp.ernet.in

A. Bisoi
e-mail: alfabisoi@gmail.com

J. Beran et al. (eds.), *Advances in Mechanism Design II*,
Mechanisms and Machine Science 44, DOI 10.1007/978-3-319-44087-3_22

useful for modelling multi-disciplinary systems and has been used in the past for motor-rotor interaction modelling [5].

2 Model Description

Here, dynamics of a system with a 3-phase squirrel cage motor (see Fig. 1) attached with an unbalanced disk mounted on a flexible foundation is studied.

The disk's mass centre at C is at distance e from the geometric centre of disk at G. The total mass of the disk is denoted by m. The geometric centre of the disk is coupled with the motor and the rotor is supported by a bearing offering constant viscous resistance R_b. The foundation is flexible. The mass, stiffness and damping coefficients of the foundation are M, K_f and R_f, respectively. Parameters considered for this system are listed in Table 1.

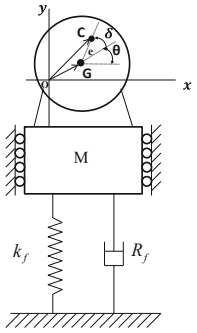

Fig. 1 Motor on a flexible foundation

Table 1 The system parameters, their descriptions and values

Parameter	Description	Value
K_f	Stiffness coefficient of foundation	15×10^4 N/m
R_f	Damping coefficient of foundation	100 Ns/m
K_{pad}	Stiffness coefficient of pad	1×10^{10} N/m
R_{pad}	Damping coefficient of pad	1×10^3 Ns/m
m	Mass of the disk	8 kg
M	Total mass of the foundation	20 kg
I_p	Polar moment of inertia of disk	0.1 kgm^2
e	Eccentricity in rotor disk	0.005 m
R_b	Bearing rotational damping coefficient	0.0002 Nms/rad
R_s	Stator resistance	0.55 Ω
R_r	Rotor equivalent resistance	0.568 Ω
I_s	Stator coil inductance	0.0048 H
I_r	Rotor equivalent inductance	0.0025 H
L_m	Mutual induction	0.1 H
T_L	Initial load torque	0.01 Nm

2.1 Equations of Motion

Let the position of the mass center G be (x_m, y_m) and geometric center C be (x, y). It follows from Fig. 1 that $y_m = y + e\sin(\theta + \delta)$ and $\dot{y}_m = \dot{y} - e\cos(\theta + \delta)\dot{\theta}$ where, $\theta = \omega t$ is the angle between the x-axis and the line passing from the geometric centre through the mass centre of the rotor, ω is the rotor speed, and δ is an arbitrary phase angle. The equations of motion of the system may be written as (2, 3, 5)

$$(M+m)\ddot{y} + R_f\dot{y} + K_f y = me\omega^2\cos(\omega t) + me\ddot{\theta}\sin(\omega t) \tag{1}$$

$$I_p\ddot{\theta} = T(\dot{\theta}) - R_b\dot{\theta} + me\ddot{y}\sin(\theta) \tag{2}$$

where $T(\dot{\theta})$ is the output torque from the motor. From Eq. 1, natural frequency $\omega_n = \sqrt{K_f/(M+m)}$. Substituting $y = A\cos(\omega t - \phi)$ in Eq. (1) yields

$$\tan(\phi) = \frac{\omega R_f}{K_f - (M+m)\omega^2} \quad \text{and} \quad A = \frac{me\omega^2}{\sqrt{(\omega R_f)^2 + \left(K_f - (M+m)\omega^2\right)^2}} \tag{3}$$

where A is the vibration amplitude of the foundation and ϕ is a phase.

Bond graph modelling of the system

An existing model of three phase six pole induction motor is used here (5). According to Maxwell-Faraday equation

$$\nabla \times E_s = \left(-\frac{\partial B}{\partial t}\right) \text{ as seen from stator} \quad \nabla \times E_r = \left(-\frac{\partial B}{\partial t}\right) \text{ as seen from rotor} \tag{4}$$

where E_s and E_r are stator electric field and rotor electric field, respectively, B is the magnetic field, and Φ is the magnetic flux. For number of turns n_s, we get potential differences (5) across terminals as

$$\begin{aligned} V_{1s} &= -n_s\dot{\Phi}_{1s}, \quad V_{2s} = -n_s\left(\dot{\Phi}_{2s}\cos\frac{2\pi}{3} + \dot{\Phi}_{3s}\sin\frac{2\pi}{3}\right), \\ V_{3s} &= -n_s\left(\dot{\Phi}_{2s}\cos\frac{4\pi}{3} + \dot{\Phi}_{3s}\sin\frac{4\pi}{3}\right) \end{aligned} \tag{5}$$

Three phase voltage supply and delta connection sub-models which are used in the integrated model are shown in Figs. 2 and 3, respectively. Here, TF moduli $\mu_{d1} = \cos\omega t$, $\mu_{d2} = \cos(\omega t - 2\pi/3)$ and $\mu_{d3} = os(\omega t - 4\pi/3)$.

In Fig. 3, e/o and e/i are the output and input voltage ports. The integrated bond graph model of the squirrel cage induction motor attached with an unbalance rotor placed on a flexible foundation is shown Fig. 4 where i_α and i_β are the currents in

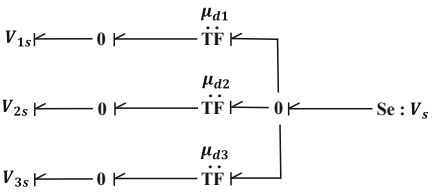

Fig. 2 The 3-phase supply sub-model

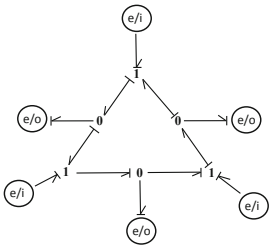

Fig. 3 Delta connection sub-model

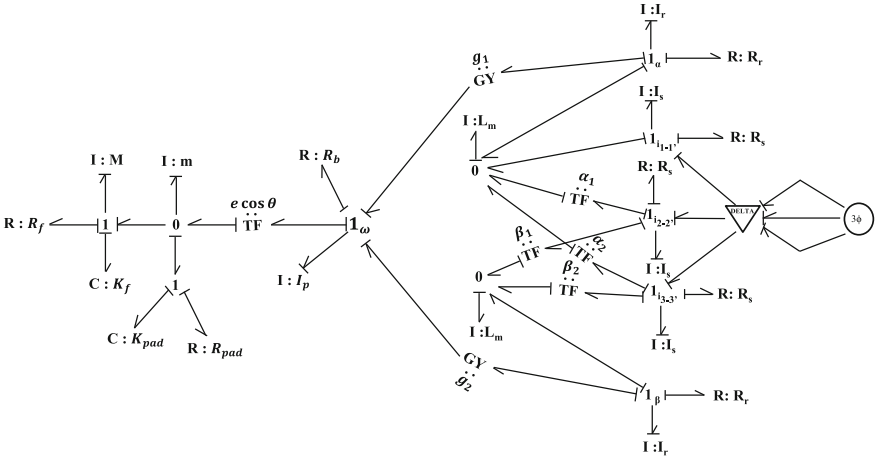

Fig. 4 Integrated bond graph model

the rotor in x and y directions, $i_{1-1'}$, $i_{2-2'}$ and $i_{3-3'}$ are the currents in the 3 different phases of stator side. The equivalent rotor inductance equivalent rotor resistance are reduced as $I_r = (n_s/n_r)^2 I_{r'}$ and $R_r = (n_s/n_r)^2 R_{r'}$ where $I_{r'}$ and $R_{r'}$ are actual rotor inductance and actual rotor resistance of the motor, respectively, and n_s and n_r are number of stator and rotor poles. In case of squirrel cage induction motors, $n_s = n_r$. Three phase voltage supply to two phase supply transformation is given as

$$\begin{bmatrix} i_{\alpha r} \\ i_{\beta r} \end{bmatrix} = \frac{\sqrt{2}}{\sqrt{3}} \begin{bmatrix} \cos 0 & \cos 2\pi/3 & \cos 4\pi/3 \\ \sin 0 & \sin 2\pi/3 & \sin 4\pi/3 \end{bmatrix} \begin{bmatrix} i_{s1} \\ i_{s2} \\ i_{s3} \end{bmatrix} \tag{6}$$

Thus, the values of transformer moduli used in bond graph model are $\alpha_1 = \sec 2\pi/3$, $\beta_1 = \csc 2\pi/3$, $\alpha_2 = \sec 4\pi/3$, $\beta_2 = \csc 4\pi/3$. Contribution of voltage from mutual inductance is modeled by GY elements. Moduli of Gyrators are given as $g_1 = L_m di_\beta/dt$ and $g_2 = L_m di_\alpha/dt$. More details of this model are available in (4, 5).

Simulation results

Using the data in Table 1, $\omega_n = 73.1$ rad/s. The variables used to plot the results are normalized transverse displacement of foundation $A^* = 2\omega_n^2 A/(\pi^2 g)$ and normalized shaft spin speed $\omega^* = \omega/\omega_n$, where g is the acceleration due to gravity. For supply voltage V_s = 53.3 V and frequency 60 Hz (377 rad/s), the rotor speed gets stuck at the resonance as shown in Fig. 5. The corresponding results for V_s = 53.4 V are shown in Fig. 6, where vibration amplitude reduces and rotor speed jumps to near synchronous speed (372 rad/s).

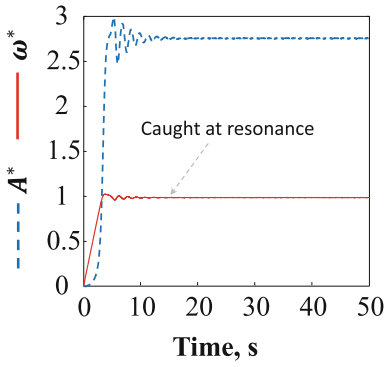

Fig. 5 Transient response during coasting up for V_s = 53.3 V

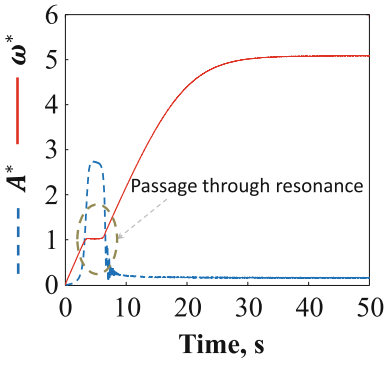

Fig. 6 Transient response during coasting up for V_s = 53.4 V

3 Speed Control of Induction Motor

Generally there are two types of speed control methods for induction motor. One is scalar control and the other is vector control method. Volts-per-hertz, commonly called V/f is the most popular method of IM control. It is widely used in industrial and domestic applications. In pure V/f approach, the voltage and frequency ratio is kept constant; the constant being specified according to motor rating in order to avoid coil burnout. Some transient simulations with V/f control of IM are shown in Figs. 7 and 8 with V/f constant chosen as 1 (f is in rad/s). In Fig. 7, the reference speed is 60 rad/s, supply voltage V_s = 60 V. The simulation results show that the motor speed reaches nearly the synchronous speed. Similar result is obtained when the reference speed is set to 80 rad/s (V_s = 80 V) and the steady speed reached is nearly the synchronous speed as shown in Fig. 8. Thus, the resonance is passed without the system being caught at it.

When the reference speed is kept just above the resonance speed, the response does not settle to any steady value. This happens due to Sommerfeld effect which excludes some speed zones from stable operation. Such cases for reference speed of 74 rad/s (resonance is at 71.3 rad/s) are shown in Figs. 9 and 10.

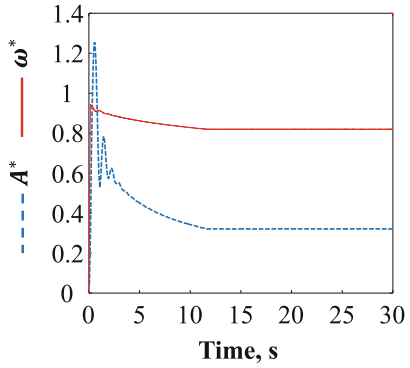

Fig. 7 Transient response during coasting up for reference speed of 60 rad/s

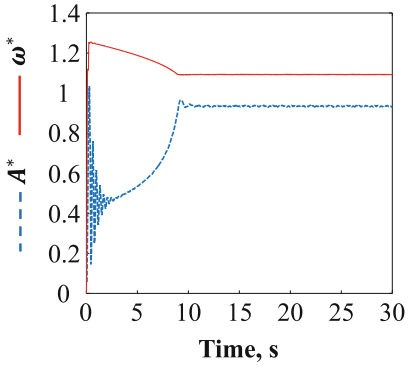

Fig. 8 Transient response during coasting up for reference speed of 80 rad/s

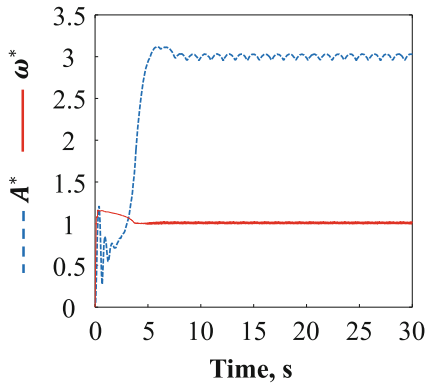

Fig. 9 Transient response during coasting up for reference speed of 74 rad/s

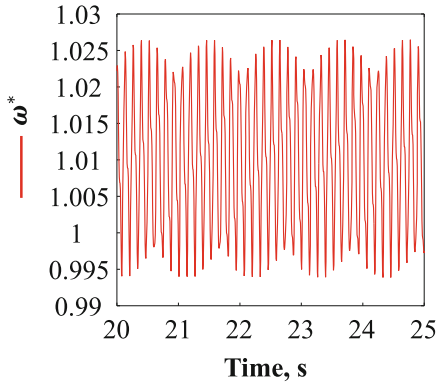

Fig. 10 A zoomed part of rotor speed response at reference speed of 74 rad/s

4 Conclusions

Many engineering applications require speed control of unbalanced rotors driven by induction motors. One example is a heavy-duty vibration generator where use of peizo-elements can be expensive. We show that passage through resonance can be a problem by simple voltage variation approach due to the existence of Sommerfeld effect. The v/f speed controller is shown to be able to regulate the rotor speed even in the regimes near the structural resonance.

References

1. Sommerfeld, A.: Beiträge Zum Dynamischen Ausbau Der Festigkeitslehe, Physikal Zeitschr **3**, 266 (1902)
2. Samantaray, A.K.: Steady-state dynamics of a non-ideal rotor with internal damping and gyroscopic effects. Int. J. Non-Linear Mech. **56**(4), 443 (2008)

3. Karthikeyan, M., Bisoi, A., Samantaray, A.K., Bhattacharyya, R.: Sommerfeld effect characterization in rotors with non-ideal drive from ideal drive response and power balance. Mech. Mach. Theory **91**, 269 (2015)
4. Mukherjee, A., Karmakar, R., Samantaray, A.K.: Bond graph in modeling, simulation and fault identification. CRC Press (2012)
5. Mukherjee, A., Karmakar, R., Samantaray, A.K.: Modelling of basic induction motors and source loading in rotor-motor systems with regenerative force field. Simul. Pract. Theor. **7**, 563 (1999)